Chemistry–A European Journal
Research Article
doi.org/10.1002/chem.202202435
Chemistry Europe
European Chemical Societies Publishing
www.chemeurj.org

Microporous Framework (Nb, Fe)-Silicate with Much Potential to Remove Rare-Earth Elements from Waters

Zhi Lin,*[a] Daniela Tavares,[b] Eduarda Pereira,[b] and João Rocha*[a]

Abstract: Nanoparticles of a new small-pore metal silicate formulated as $Na_{2.9}(Nb_{1.55}Fe_{0.45})Si_2O_{10}\cdot xH_2O$ and exhibiting the structure of previously reported $Rb_2(Nb_2O_4)(Si_2O_6)\cdot H_2O$ have been synthesized under mild hydrothermal conditions. Replacement of the bulky Rb^+ by smaller Na^+ ions was accomplished by stabilizing the framework structure via partial occupancy of the Nb^{5+} sites by Fe^{3+} ions. Exploratory ion-exchange assays evidence the considerable potential of this new silicate to remove rare-earth elements from aqueous solutions.

Introduction

Microporous zeolite-like silicates have been widely used as catalysts, ion exchangers and in gas sorption and separation because they exhibit uniformed micropore size, high surface area, large pore volume and good thermal and hydrothermal stability. The synthesis of silicates bearing transition metals, main group elements and lanthanides broadens the field and scope of application of zeolitic materials. In particular, silicates with stoichiometric amounts of titanium, zirconium and vanadium, usually in five- or six-fold coordination, have raised much interest.[1,2] Other microporous metal silicates, including niobium silicates, are comparatively much less studied.[3–6]

The synthesis of the analogue of nenadkevichite, the mineral $(Na,Ca)(Nb,Ti)Si_2O_7\cdot 2H_2O$ that is part of the labuntsovite supergroup, has been reported twenty years ago.[7] The structure of nenadkevichite consists of corner-sharing octahedra forming -Nb-O–Nb-O- chains that are connected by square rings of tetrahedra Si_4O_{12}. In synthetic nenadkevichite, the potassium and sodium cations, and H_2O molecules reside in the pores and channels. The mineral labuntsovite has the same atomic arrangement but crystallizes in a different space group, and contains Ti and a small amount of Nb. The pure Ti analogue was first synthesized in 1996.[7] The labuntsovite supergroup encompasses some 30 members, for example, minerals organovaite and vuoriyarvite, with a highest Nb occupation of the TO_6 site of ca. 90%. The pure Nb form has not yet been found in nature nor prepared in the laboratory. The structure of the mineral komarovite, $(Na,K,Ca)_4(Nb,Ti)_3Si_2O_{13}F\cdot 2H_2O$, consists of corner-sharing octahedra -Nb-O–Nb-O- chains along [100] and [001] directions interconnected by corner-sharing to form a triple layer in *ac* plane. These niobium-bearing layers are connected by square rings of tetrahedra, Si_4O_{12}, forming a three-dimensional framework structure.[8] In 2008, Lii et al. synthesized a new niobium silicate, $Rb_2(Nb_2O_4)(Si_2O_6)\cdot H_2O$, via a high-temperature (600 °C), high-pressure (ca. 170 MPa), hydrothermal reaction.[6] The structure of this material also comprises corner-sharing octahedra -Nb-O–Nb-O- chains along two perpendicular directions, interconnected by corner-sharing to form a double layer. The niobium layers are connected by square rings of tetrahedra, Si_4O_{12}, forming a three-dimensional framework structure. Few other open framework niobium silicates have been prepared. For example, a sodium niobium tetrasilicate, $Na_2H(NbO)Si_4O_{11}\cdot 1.25H_2O$, was prepared and transformed to the proton form and to the partially-exchanged cesium form.[4] AM-11 (structure still unknown) catalyzes the dehydration of tertbutyl alcohol to isobutene with high activity and selectivity.[3] NSH-1, $[(C_4N_2H_{11})Nb_3SiO_{10}]$, an organically-templated niobium silicate, has a three-dimensional framework consisting of a network of interconnecting six-ring and eight-ring channels. Two parallel corner-sharing octahedra -Nb-O–Nb-O- chains interconnect by sharing edges, and are further connected by corner-sharing polyhedra -Nb-O–Si-O–Nb-O–Si-O- chains.[9] Clearfield and co-workers reported the synthesis of $Na_2Nb_4Si_2O_{15}\cdot 4H_2O$ and $Na_2Nb_8Si_4O_{29}\cdot 18H_2O$ for cesium and strontium removal[10] and a few other niobium silicates of alkaline, alkaline-earth and other divalent metals with unknown structures.[11]

Coming back to the niobium silicate $Rb_2(Nb_2O_4)(Si_2O_6)\cdot H_2O$ of Lii et al., both the high temperature (600 °C) of the hydrothermal synthesis, and the presence of expensive rubidium, limit its application.[6] It is, thus, of interest to prepare an

[a] Dr. Z. Lin, Prof. J. Rocha
Department of Chemistry
CICECO - Aveiro Institute of Materials
University of Aveiro
3810-193 Aveiro (Portugal)
E-mail: zlin@ua.pt
rocha@ua.pt

[b] Dr. D. Tavares, Prof. E. Pereira
Department of Chemistry
LAQV-REQUIMTE - Associated Laboratory for Green Chemistry
University of Aveiro
3810-193 Aveiro (Portugal)

Supporting information for this article is available on the WWW under https://doi.org/10.1002/chem.202202435

isostructural material not containing rubidium. We have reasoned that since Na^+ is much smaller than Rb^+, the presence of more Na^+ in the channels is required to stabilize the framework. If so, the excess Na^+ positive charge may be compensated for by reducing the charge of the framework metals, for example, replacing Nb^{5+} by M^{4+} or M^{3+} ions of similar size. Furthermore, M^{4+} or M^{3+} must be amenable to form corner-sharing octahedral chains. To explore this idea, we have chosen Fe^{3+}, and here we wish to report the synthesis and characterization of a Rb-free, Fe-substituted, microporous niobium silicate with composition $Na_{2.9}(Nb,Fe)_2Si_2O_{10}.xH_2O$, exhibiting the $Rb_2(Nb_2O_4)(Si_2O_6)\cdot H_2O$ structure (henceforth dubbed **1**).

Rare-earth elements (REE) comprise the lanthanide series plus scandium and yttrium, and find use in many consumer products, such as cellular telephones, computer hard drives, electric and hybrid vehicles, screen monitors and televisions, fluorescent lamps, and permanent magnets.[12] At the end of their life, these products are often disposed of without any treatment leading to an increase in the high levels of contamination.[13,14] Nevertheless, this critical issue is combined with the significant content of REE, which makes them a potential secondary source of such elements. In this regard, the extraction of REE from e-waste is receiving much attention.[15] Processes like sorption on different types of sorbents for remediation, or recovery of REE from aqueous solutions are promising alternatives to other conventional methods.[16–18] Here, we assess the potential of **1** to remove a mixture of REE from aqueous solutions. The sorption capacity of the sorbent was tested using a natural water.

Results and Discussion

Attempting to synthesize a material with composition $Na_{2.9}(Nb,Fe)_2Si_2O_{10}\cdot xH_2O$ with the structure of material **1**, reaction mixtures with a nominal Fe/Nb molar ratio in the range 0.17–0.43, and ensuing Na content, were prepared. The effect of the water content, pH, synthesis time and temperature on the products obtained was also assessed. Samples of good phase purity could only be obtained in the presence of fluoride ions which, however, did not end up in the final solid. The obtained samples display very similar powder XRD patterns (Figure 1). The best sample (regarding phase purity and crystallinity) was prepared as described in the Experimental Section and had a nominal gel Fe/Nb molar ratio of 0.32. The composition of this sample (as ascertained by ICP-MS) is $Na_{2.9}(Nb_{1.55}Fe_{0.45})Si_2O_{10}\cdot xH_2O$ (henceforth dubbed **2**). SEM (Figure 2) shows that this sample consists of aggregates of small crystallite bars ca. 50 nm in width and 200–300 nm in length.

TGA indicates that the material reversibly loses the pore water molecules between ca. 100 and 400 °C (ca. 6 wt% loss), although below 100 °C samples may exhibit different amounts of (physiosorbed) water (Figure 3). As witnessed by powder XRD, the material is stable until ca. 500 °C (Figure 4).

The FT-Raman spectra of **2** and synthetic Nb-bearing nenadkevichite are shown in Figure 5. The latter exhibits two

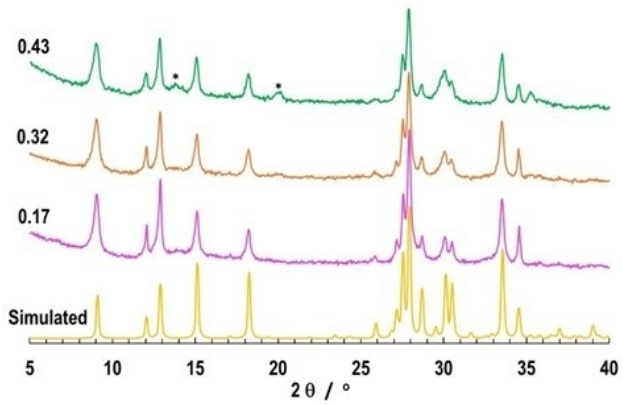

Figure 1. Powder X-Ray Diffraction patterns of $Na_{2.9}(Nb_{1.55}Fe_{0.45})Si_2O_{10}.xH_2O$ samples synthesized from gels with the nominal Fe content 0.17, 0.32 and 0.43. A simulated pattern is also shown (assuming: $Rb_2(Nb_2O_4)(Si_2O_6)\cdot H_2O$ structure, 17% of the Nb^{5+} site was occupied by Fe^{3+}, and full replacement of Rb^+ by Na^+). The stars depict impurity reflections.

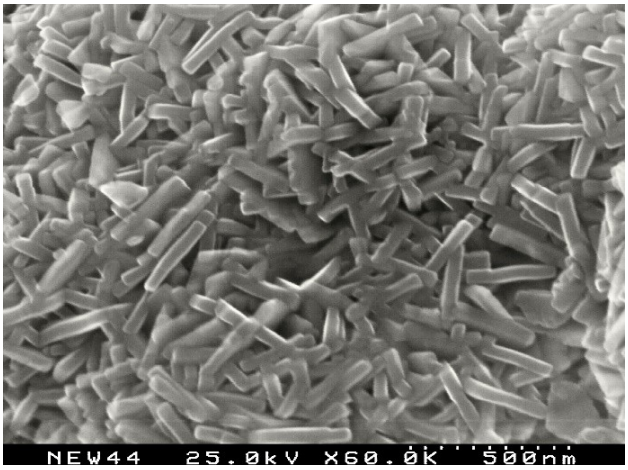

Figure 2. Scanning Electron Microscopy image of $Na_{2.9}(Nb_{1.55}Fe_{0.45})Si_2O_{10}\cdot xH_2O$.

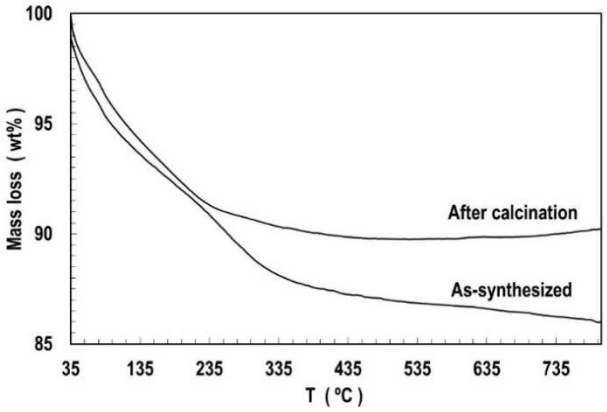

Figure 3. Thermogravimetric Analysis traces of as-synthesized and rehydrated $Na_{2.9}(Nb_{1.55}Fe_{0.45})Si_2O_{10}\cdot xH_2O$ after calcination.

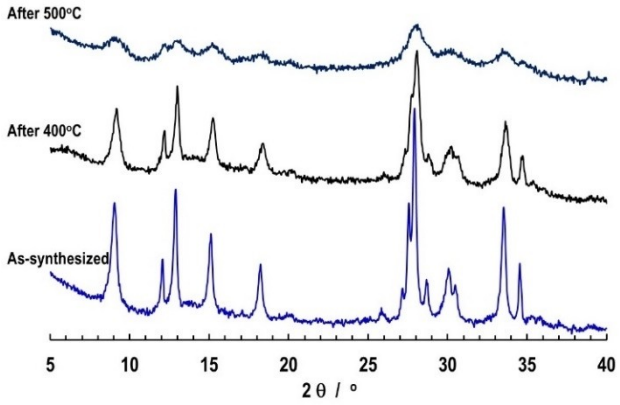

Figure 4. Powder X-Ray Diffraction patterns of $Na_{2.9}(Nb_{1.55}Fe_{0.45})Si_2O_{10}{\cdot}xH_2O$: as-prepared, after calcination at 400 °C for 2 h, and at 500 °C for 4 h.

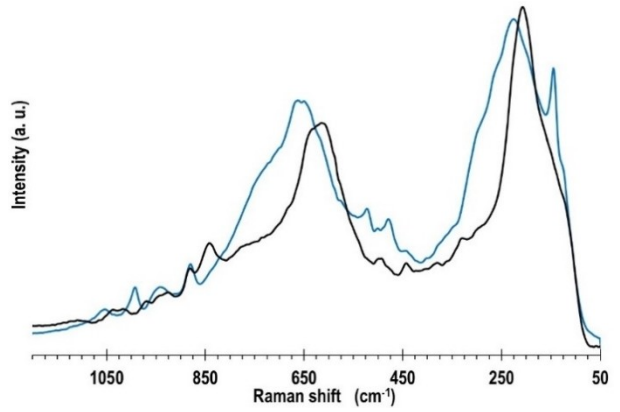

Figure 5. Fourier-Transform Raman spectra of $Na_{2.9}(Nb_{1.55}Fe_{0.45})Si_2O_{10}{\cdot}xH_2O$ (black line) and synthetic analogue of Nb-bearing silicate nenadkevichite (blue line).

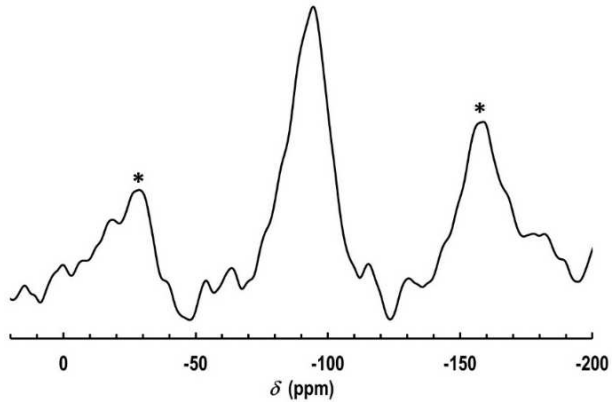

Figure 6. ^{29}Si Magic-Angle Spinning Nuclear Magnetic Resonance spectrum of $Na_{2.9}(Nb_{1.55}Fe_{0.45})Si_2O_{10}{\cdot}xH_2O$. Asterisks depict spinning sidebands.

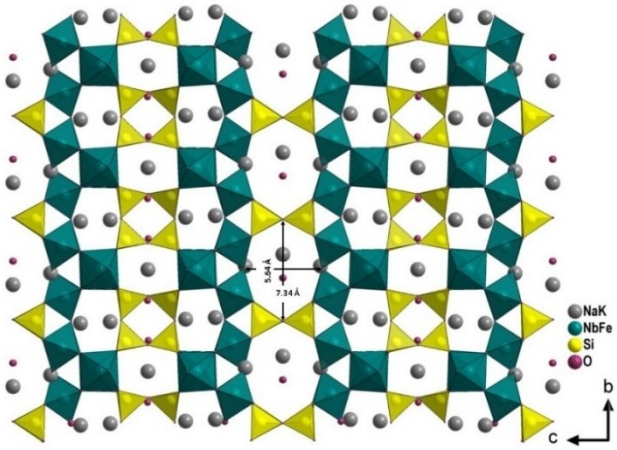

Figure 7. Schematic representation of the structure of $Na_{2.9}(Nb_{1.55}Fe_{0.45})Si_2O_{10}{\cdot}xH_2O$ viewed along the *a*-axis.

main bands at 226 and 668 cm^{-1}, which have been ascribed to the NbO_6 octahedra.[7] Sample **2** also displays two main bands in similar ranges, at 209 and ca. 625 cm^{-1}, indicating the presence of NbO_6 octahedra.

The ^{29}Si MAS NMR spectrum of **1** displays a single resonance at −95.9 ppm ascribed to Q^4(2 Nb) units (Si bonded via oxygen atoms to 2 Si and 2 Nb atoms).[6] Synthetic Nb-bearing nenadkevichite, in turn, exhibits a main peak at −91 ppm also assigned to Q^4(2 Nb) environments.[7] **2** shows a broad peak at ca. −95 ppm (flanked by strong spinning sidebands, due to the presence of paramagnetic Fe^{3+}) (Figure 6) suggesting the presence of Q^4(2 Nb) species.

Powder XRD confirms **2** and the rubidium niobium silicate **1** are isostructural (Figure 1), with partial occupancy of the Nb^{5+} site by Fe^{3+} and the full replacement of Rb^+ by Na^+ (and a minor amount of K^+). A schematic representation of the structure proposed for **2** viewed along the *a*-axis is depicted in Figure 7. The SiO_4 tetrahedron shares corners with two NbO_6 octahedra and two SiO_4 tetrahedra, in accord with the FT-Raman and ^{29}Si MAS NMR evidence.

We have investigated the potential of **2** to remove from water a mixture of Ce, La, Y, Nd, Pr, Eu, Gd, Tb and Dy at an equimolar concentration of 1 μmol/L. In each experiment, the residual REE concentration in water was evaluated at different contact times. The variation of normalized concentration was obtained from the residual REE concentration in water. The uptake of REE from spiked ultra-pure water is an important first step to evaluate the material's capacity under simple matrix conditions. To assess the REE removal capacity of **2** in the presence of a more complex matrix, next we have used natural mineral water spiked with REE.

Figure 8 shows the normalized concentration curves of each REE for both, spiked ultra-pure water, and spiked mineral natural water, with time. The normalized REE concentration of in solution decreases with time and the removal profile is quite similar for both matrices. This decrease is due to REE uptake by the material because the corresponding controls do not show such behavior. The slopes of the removal curves indicate that increasing the complexity of the matrix from ultra-pure water to mineral natural water does not change REE removal. *Ca.* 78% of

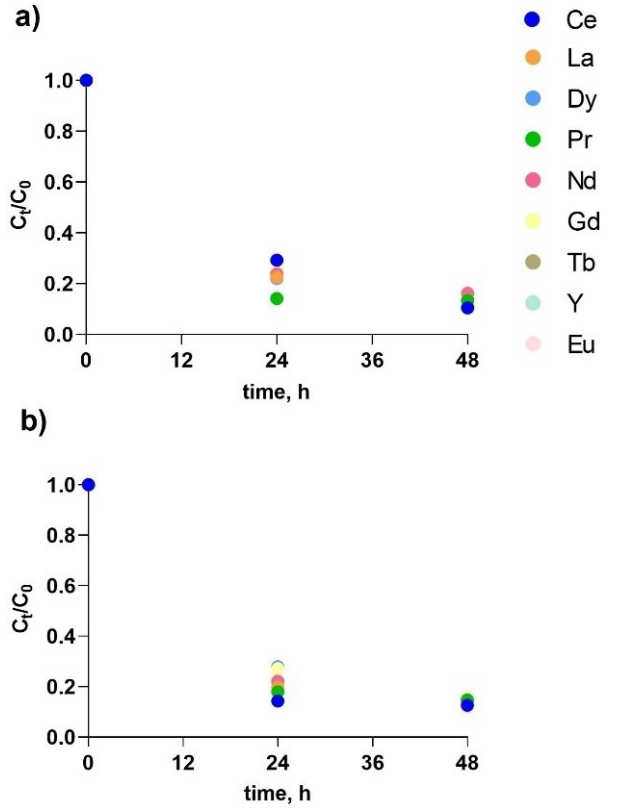

Figure 8. Time profile of normalized rare-earth elements concentration in a) ultra-pure water, and b) natural mineral water, using 100 mg/L of $Na_{2.9}(Nb_{1.55}Fe_{0.45})Si_2O_{10}{\cdot}xH_2O$, C_{REE} of 1 μmol/L and pH 6.

all elements were removed from pure water after 24 h and 82% after 48 h. For spiked mineral natural water, the removal was ca. 76% after 24 h and 86% after 48 h.

Concerning the REE removal process, the mass of material **2** is an important parameter as forthcoming from Figure 9. For mineral natural water, a mass of 20 mg/L removed some 80%

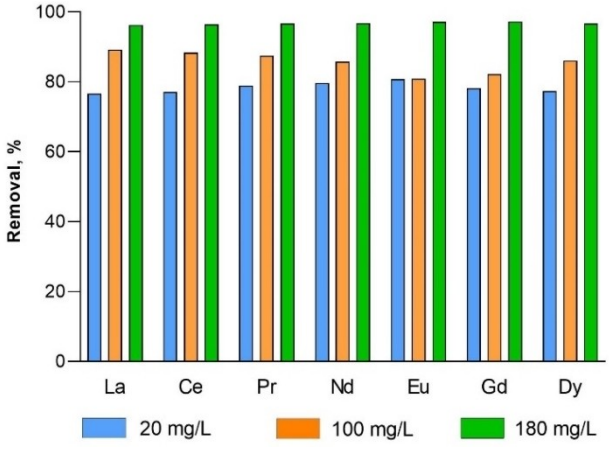

Figure 9. Removal percentage of rare-earth elements from natural mineral water using different absorbent masses, C_{REE} of 1 μmol/L, 48 h and pH 6.

of the REE mixture. Increasing the mass from 20 to 180 mg/L increased the REE removal to ca. 100%.

Conclusions

Nanoparticles of a new small-pore metal silicate formulated as $Na_{2.9}(Nb_{1.55}Fe_{0.45})Si_2O_{10}{\cdot}xH_2O$ (**2**) and exhibiting the structure of (**1**) have been synthesized under mild hydrothermal conditions. Replacement of the bulky Rb^+ by smaller Na^+ ions required stabilizing the framework via partial occupancy of the Nb^{5+} sites by Fe^{3+} ions. Powder XRD, FT-Raman and ^{29}Si MAS NMR support the proposed crystal structure, which is stable up to almost 500 °C. Ion exchange assays show the considerable potential of **2** to remove REE from aqueous solutions.

Experimental Section

Chemicals: The reagents used in syntheses are sodium silicate solution (25.5–28.5 wt.% SiO_2, 7.5–8.5 wt.% Na_2O, Merck), NaOH (Merck), NaCl (Panreac), KCl (99 wt%, Panreac) and $FeCl_3$ (99 wt%, Merck). All chemicals used in the rare-earth elements (REE) removal experiments were of analytical reagent grade and were used without further purification. The REE (Ce, La, Y, Nd, Pr, Eu, Gd, Tb, Dy) certified standard solutions (1000 mg/L, in 1.4%–7% HNO_3) were acquired from Inorganic Ventures. Nitric acid (65%) and sodium hydroxide (>99%) were purchased from Merck. Prior to use, all glassware was acid-washed with HNO_3 25% for 24 h and then rinsed with ultra-pure water.

Synthesis: The chemical composition (molar ratios) of the initial gel was 7.53 Na_2O:1.86 K_2O : 5.87 SiO_2 : 0.43–0.32 Nb_2O_5 : 0.07–0.18 Fe_2O_3 : 192–214 H_2O. In a typical synthesis, the precursor gel was prepared as follows. 8.01 g of sodium silicate solution, 2.53 g of sodium hydroxide, 0.5 g of sodium chloride, 0.42 g of potassium chloride and 1.00 g of potassium fluoride were thoroughly dissolved in 16 mL of water. A mixture of 1.26 g of niobium pentachloride and 0.24 g of iron trichloride was added to this solution with stirring. This was followed by alternating ultra-sonication and stirring steps until a homogeneous gel was obtained. At this point the pH was 11.7 (pH after 1:100 dilution with water). The resulting precursor gel, with the molar composition 7.53 Na_2O:1.86 K_2O:5.87 SiO_2:0.38 Nb_2O_5:0.12 Fe_2O_3:192 H_2O, was then heated in Teflon lined autoclaves at 230 °C for 7 days, under autogenous pressure without agitation. The solid product was collected by centrifugation, and washed thoroughly at room temperature with distilled water, and dried at 80 °C. The final product is a light-yellow nanocrystalline powder.

Characterization: Powder X-Ray Diffraction (XRD) data were collected at room temperature on a PANalytical Empyrean diffractometer in a Bragg-Brentano geometry using Cu$K\alpha$ X-radiation, in the 2θ range 5°–40°. The unit cell parameters were refined using programme Powder Cell.[19] Scanning Electron Microscopy (SEM) images and Energy Dispersive X-ray Spectrometry (EDS) were carried out on a Hitachi S-4100 microscope equipped with a RONTEC UHV Dewar Detektor and EDS system. Fourier-Transform (FT) Raman spectra were collected on a Bruker RFS 100/S spectrometer using a Nd:YAG laser (1064 nm) in the range of 50–4000 cm^{-1}, with a resolution of 2 cm^{-1}. ^{29}Si Magic-Angle Spinning (MAS) Nuclear Magnetic Resonance (NMR) spectra were recorded at 79.49 MHz on a Bruker Avance III 400 (9.4 T) wide-bore spectrometer, with a spinning rate of 5 kHz and 60 s recycle delays. Chemical shifts are quoted in ppm from tetramethylsilane (TMS). Thermogra-

vimetric Analysis (TGA) was measured on a Shimadzu TGA-50 analyzers under air with a heating rate of 5 °C per minute. Before measurement, the samples were fully hydrated.

Removal of REE from water: The ability of the materials to remove from water a mixture of REE (Ce, La, Y, Nd, Pr, Eu, Gd, Tb, Dy) was evaluated by contacting this material with water with a known REE concentration, for variable periods of time. The removal experiments were carried out in batch conditions using 1000 mL volumetric flasks and under magnetic stirring. Water with a mixture of REE in equimolar concentration of 1 μmol/L for each element was prepared daily by diluting the corresponding stock solution in ultra-pure water (18 MΩ/cm). The pH of all REE solutions was adjusted to 6 using 1–10 mol/L NaOH.

An amount of 100 m/L of material was added to the water and this moment was considered the starting point of the experiment. During all the experiment, the REE solution was stirred continuously. Aliquots were withdrawn at increasing contact times at 0, 24 and 48 h. Before REE determination, water samples were centrifuged at 50,000 rpm for 3 minutes, then acidified to pH below 2 with concentrated nitric acid.

In order to assess the performance of the material with a more real-world contaminated water matrix, experiments were performed using natural mineral (composition given in Supporting Information) water spiked with the REE mixture. Equimolar concentration of 1 μmol/L of each REE was again used. Control experiments, i.e., REE solutions in the absence of porous material, were performed in parallel and under the same experimental conditions.

REE removal efficiency was calculated using Equation (1):

$$\text{Removal } (\%) = \frac{(C_0 - C_t)}{C_0} \times 100 \quad (1)$$

where C_0 is the initial REE (mg/L) concentration, and C_t the REE concentration at time *t*.

Quantification of REE: The quantification of REE (Ce, La, Y, Nd, Pr, Eu, Gd, Tb and Dy) in waters was performed by Inductively Coupled Plasma Mass Spectrometry (ICP-MS) on a Quadrupole Thermo Scientific X Series spectrometer. Calibration curves were elaborated with concentrations ranging from 0.1 to 10 μg/L, diluted from a multi-element certified standard solution for ICP analysis (IV-ICPMS 71A). Curves with correlation coefficients under 0.999 were discarded and the error associated with each standard and duplicates never exceeded 10%.

Author contributions

ZL: conceptualization of material synthesis, characterization, writing the manuscript. JR: discussion of results, writing the manuscript. DT, EP: conducting REE removal experiments, writing the manuscript.

Acknowledgements

The researchers acknowledge the project CICECO-Aveiro Institute of Materials, UIDB/50011/2020, UIDP/50011/2020 & LA/P/0006/2020 and the financial support of REQUIMTE, UIDB/50006/2020, financed by national funds through the Portuguese Foundation for Science and Technology/MCTES. The NMR spectrometers are part of the National NMR Network (PT NMR) and are partially supported by Infrastructure Project No. 022161 (co-financed by FEDER through COMPETE 2020, POCI and PORL and FCT through PIDDAC).

Conflict of Interest

The authors declare no conflict of interest.

Data Availability Statement

The data that support the findings of this study are available from the corresponding author upon reasonable request.

Keywords: hydrothermal synthesis · microporous · niobium silicate · rare earth removal · silicate

[1] J. Rocha, D. Ananias, F. A. A. Paz, Comprehensive Inorganic Chemistry II (Second Edition), From Elements to Applications, Vol. 4, Solid-State Materials, Including Ceramics and Minerals, Editors-in-Chief: Jan Reedijk and Kenneth Poeppelmeier, Elsevier, Amsterdam, **2013**, 87–110.
[2] Z. Lin, F. A. A. Paz, J. Rocha, in Layered Mineral Structures and Their Application in Advanced Technologies, *EMU Notes in Mineralogy* **2011**, *11*, 123–149.
[3] J. Rocha, P. Brandão, A. Phillippou, M. W. Anderson, *Chem. Commun.* **1998**, 2687–2688.
[4] M. A. Salvadó, P. Pertierra, S. García-Granda, S. A. Khainakov, J. R. García, A. I. Bortun, A. Clearfield, *Inorg. Chem.* **2001**, *40*, 4368–4373.
[5] A. S. Dias, S. Lima, P. Brandão, M. Pillinger, J. Rocha, A. A. Valente, *Catal. Lett.* **2006**, *108*, 179–186.
[6] J.-M. Tasi, P.-T. Tu, T.-Sh. Chan, K.-H. Lii, *Inorg. Chem.* **2008**, *47*, 11223–11227.
[7] J. Rocha, P. Brandão, Z. Lin, A. P. Esculcas, A. Ferreira, *J. Phys. Chem.* **1996**, *100*, 14978–14983.
[8] T. Balić Zunić, O. V. Petersen, H. J. Bernhardt, H. I. Micheelsen, *Neues Jahrb. Mineral. Monatsh.* **2002**, *11*, 497–514.
[9] R. J. Francis, A. J. Jacobson, *Angew. Chem. Int. Ed.* **2001**, *40*, 2879–2881; *Angew. Chem.* **2001**, *113*, 2963–2965.
[10] A. I. Bortun, L. N. Bortun, A. Clearfield, *Solvent Extr. Ion Exch.* **1997**, *15*, 909–929.
[11] A. I. Bortun, L. N. Bortun, S. A. Khainakov, A. Clearfield, C. Trobajo, J. R. Garcia, *Solvent Extr. Ion Exch.* **1999**, *17*, 649–675.
[12] V. Balaram, *Geosci. Front.* **2019**, *10*, 1285–1303.
[13] A. Brewer, I. Dror, B. Berkowitz, *Chemosphere* **2022**, *287*, 132217.
[14] R. K. Jyothi, T. Thenepalli, J. W. Ahn, P. K. Parhi, K. W. Chung, J. Y. Lee, *J. Cleaner Prod.* **2020**, *267*, 122048.
[15] R. K. Jyothi, *Rare-Earth Metal Recovery for Green Technologies: Methods and Applications*; Springer Cham, **2020**.
[16] I. Anastopoulos, A. Bhatnagar, E. C. Lima, *J. Mol. Liq.* **2016**, *221*, 954–962.
[17] E. Allahkarami, B. Rezai, *Process Saf. Environ. Prot.* **2019**, *124*, 345–362.
[18] X. D. Zheng, C. Wang, J. D. Dai, W. D. Shi, Y. S. Yan, *J. Mater. Chem. A* **2015**, *3*, 10327–10335.
[19] W. Kraus, G. Nolze, *J. Appl. Crystallogr.* **1996**, *29*, 301–303.

Manuscript received: August 5, 2022
Accepted manuscript online: September 26, 2022
Version of record online: October 28, 2022